Carrier thermal escape and retrapping in self-assembled quantum dots

S. Sanguinetti
Istituto Nazionale per la Fisica della Materia, Dipartimento di Scienza dei Materiali, Università di Milano ''Bicocca,'' Via Cozzi 53, I-20125 Milano, Italy

M. Henini
School of Physics and Astronomy, University of Nottingham, University Park, Nottingham NG7 2RD, United Kingdom

M. Grassi Alessi and M. Capizzi
Istituto Nazionale per la Fisica della Materia, Dipartimento di Fisica, Università di Roma ''La Sapienza,'' Piazzale A. Moro 2, I-00185 Roma, Italy

P. Frigeri and S. Franchi
CNR-MASPEC Institute, Pario delle Scienze 37a, I-43010 Fontanini, Parma, Italy
(Received 22 December 1998; revised manuscript received 7 May 1999)

The effects of carrier thermal escape and retrapping on the temperature dependence of the photoluminescence of InAs/GaAs self-assembled quantum dots are investigated. A systematic experimental study of the temperature evolution of the photoluminescence spectra in two different sets of samples is reported. The photoluminescence behavior is well reproduced in terms of a steady state model for the carrier dynamics which takes into account the quantum-dot size distribution, random population effects, and carrier capture, relaxation, and retrapping. The relative contributions of these processes to the photoluminescence thermal quenching is discussed. [S0163-1829(99)07335-X]

I. INTRODUCTION

The quest for high performance optoelectronic devices has promoted a growing interest for zero-dimensional semiconductor heterostructures [or quantum dots (QDs)]. In these systems, indeed, the strong localization of the electronic wave function leads to an atomiclike electronic density of states and to the possible realization of novel and improved photonic and electronic devices.[1–3] Furthermore, the self aggregation of defect-free QDs during the epitaxial deposition of strained semiconductor layers[4] has stimulated a large number of experimental works. QD injection-laser prototypes, made from InAs/GaAs heterostructures, have now characteristics as good as quantum well based devices.[5]

A crucial issue for the realization of room temperature efficient photonic devices is the understanding of the temperature dependence of the QD photoluminescence (PL). An unusual temperature dependence of (i) the integrated intensity, (ii) the peak energy position, and (iii) the width of the PL bands in InAs/GaAs self-assembled QDs has been reported by several groups.[6–11] In particular, the emission energy of the PL bands exhibits a sigmoidal behavior and the PL band linewidth decreases with increasing temperature. Such anomalies in the PL temperature dependence cannot be explained on the basis of a direct coupling between QD states,[12] even if one introduces two activation energies (mainly to account for the high-temperature quenching of the PL bands). Moreover, the general description in terms of a carrier thermal evaporation from the QD ground state is complicated by the presence of a wetting layer (WL) connecting the QDs. Recently, the simple thermal escape model has been criticized and the critical role of the carrier capture and relaxation—as well as of their dependence on temperature—in determining the QD radiative recombination efficiency has been pointed out.[13] However, the carrier relaxation in QDs is poorly understood, in particular, the phenomenology of the carrier interlevel scattering. In the PL spectra, an emission from excited states has been observed before the emission from the ground state was saturated. This feature has been attributed to a slowdown of the interlevel scattering since the energy difference of the electronic excited states varies with QD shape and size and cannot always match the optical phonon frequencies. However, no clear evidence of a phonon bottleneck has been found, so far, in the time dependence of the PL spectra.[14–16] Moreover, it has been demonstrated that the observation of excited states in the PL spectra is possible even in the case of very fast relaxation processes like Auger-like recombination and impurity assisted relaxation.[17,18] In fact, because of the random nature of the QD population mechanism,[19] a number of QDs can show an excited state emission before the ground state is saturated in the whole QD ensemble.

In this paper, a steady-state thermal model which takes into account all the relevant thermalization and quenching processes active in QDs is proposed. This model well reproduces the temperature dependence of the PL spectrum in a large number of samples. The model is based on a simple set of rate equations connecting the QDs, the wetting layer, and the GaAs barrier states, namely, the main components of the system. It takes into account the random carrier capture by QDs,[19] the energy dispersion of the ground states, the lack of direct coupling between different QDs, and the role of the wetting layer which provides a channel for carrier exchange. In the model, the low-temperature PL spectrum provides the

 ©1999 The American Physical Society

QD density of states (DOS), while the ground state recombination time and the WL-to-QD excitation transfer time are set equal to values reported in the literature. A limited number of fitting parameters are introduced in the model. A critical discussion of the relative weight of the different phenomena involved in the recombination process is presented on the grounds of a quantitative comparison between experimental observations and model simulations.

This paper is organized in the following way. Section II is dedicated to the description of the sample preparation procedure and of the experimental setup. In Sec. III, the experimental findings and models proposed in the literature for the PL temperature dependence are briefly reviewed. Our rate equation model is presented in Sec. IV. Finally, the experimental results and the model simulations are reported and discussed in Secs. V and VI, respectively.

II. SAMPLE GROWTH AND EXPERIMENTAL DETAILS

Two different sets of samples obtained from different sources were studied. The growth procedures are summarized here. The first set of samples was grown by molecular beam epitaxy (MBE)(Varian Gen-II system) on liquid encapsulated Czochralski semi-insulating GaAs substrates with (100) $\pm 0.5°$ (sample NU1468) and (311)A/B $\pm 0.5°$ (samples NU1422 and NU1478, respectively) surfaces. The structures consisted of the substrate, a 0.3 μm thick undoped GaAs buffer followed by a $15\times(3.8$ nm $Al_{0.33}Ga_{0.67}As$ $+3.4$ nm GaAs) superlattice, a 0.2 μm undoped GaAs, 1.8 monolayers (ML) of InAs (the QD region), and, finally, a 30 nm undoped GaAs capping layer. The growth temperature ($T_g=630\,°C$) was monitored by a pyrometer, except during the growth of InAs and of the capping layer ($T_g=500\,°C$). The growth rates were 1 ML/s for GaAs, 0.5 ML/s for AlAs, and 0.066 ML/s for InAs (average thickness 1.8 ML). At the growth temperature of 630 °C, a very low As/Ga ratio (≈ 13) was chosen to achieve a (2×4) reflection high-energy-electron diffraction (RHEED) pattern during the growth on (100) surfaces. The samples were rotated during the growth to improve their uniformity. The change from a streaky to a spotty RHEED pattern has been taken as a fingerprint of the onset of the three-dimensional growth mode. After growth, the epitaxial surfaces were examined by using a Nomarski phase-contrast optical microscope and were found to be mirror smooth and nearly defect-free. The second set of samples (MA882, MA884, and MA886) have been prepared in a MBE Varian Gen-II modular system equipped with a valved cracker cell for As. The cracker stage of the cell was kept at 500 °C so that As_4 was used during epitaxial growth, with a beam equivalent pressure ratio As/Ga ≈ 17. The substrates were radiatively heated and the growth temperature was monitored by an optical pyrometer suitable for GaAs. The growth rates were 0.87 and 0.133 ML/s for GaAs and InAs, respectively. The structures consist of a semi-insulating $(100)\pm 0.25°$ GaAs substrate, a 100 nm thick GaAs buffer grown at 600 °C, a InAs deposit grown at 500 °C with a coverage ranging between 1.6 (MA882) and 3.0 ML (MA886), and a 21.5 nm thick GaAs cap layer. At the end of the buffer a growth interruption of 210 s was performed to change and stabilize the substrate temperature for the growth of the InAs dots. A very sharp (2×4) RHEED pattern was observed after this stage, which indicates a very smooth surface. During the deposition of InAs the onset from 2D to 3D growth mechanism was observed after 12.1 s, corresponding to a deposition of 1.6 ML of InAs. A second 210 s growth interruption was performed before growing the GaAs cap in order to lower T_g down to 350 °C. At this temperature 5 ML of GaAs were grown, in order to minimize the interactions between InAs and GaAs, then the temperature was raised up to 600 °C and 20 nm of GaAs were grown to complete the cap. This procedure has been shown to give high quality structures.

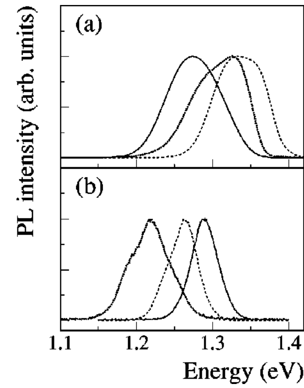

FIG. 1. PL spectra of the samples measured at $T=10$ K. (a) NU1468 (continuous line), NU1422 (short–dotted line), NU1478 (dashed line); (b) MA882 (continuous line), MA886 (short–dotted line) and MA884 (dashed line). Each spectrum is normalized to its maximum.

The PL spectra were measured using a grating monochomator. The excitation source was a multiline Ar^+ laser. The laser spot diameter ranged from 100 to 500 μm, with an excitation power density varying from a few Wcm^{-2} to some hundredths Wcm^{-2}. Measurements between 10 and 300 K were performed using a cold-finger, closed cycle He refrigerator. The low-temperature spectra of the six samples are displayed in Fig. 1.

III. QD TEMPERATURE BEHAVIOR

The experimental findings and the models developed so far to explain the complex phenomenology shown by the temperature dependence of the InAs/GaAs QD photoluminescence[6–11] are summarized in the following.

(1) The PL line of a single QD shifts with temperature as the bandgap does.[10]

(2) The PL bands of an ensemble of QDs undergo a red shift with temperature much faster than that of the InAs band gap and, sometimes, their peak energies exhibit a sigmoidal dependence on temperature.[6]

(3)In the latter case, the full width at half maximum (FWHM) is constant up to ≈ 30 K and undergoes a strong reduction (up to $\approx 50\%$) at higher temperatures. After having reached a minimum value at $T\approx 100$ K, the FWHM slowly recovers the low-T value.

(4) The spectrum of those bands which exhibit a complex structure at low-T undergoes strong changes with increasing temperature, in particular, the emission on the low-energy side of the QD band gains in intensity with respect to that on the high-energy side, at least for $T\gtrsim 30$ K.[6]

After the works of Fafard et al.[10] and Brusaferri et al.[6] the PL anomalous temperature dependence has been attributed mainly to excitation-distribution effects in the DOS of QDs with random size. In fact, the single QD emission follows well that of the InAs band gap and a carrier redistribution over DOS favors the emission on the low-energy side of the band.

In spite of this complex phenomenology, the temperature dependence of the integrated intensity of QDs is usually fitted by assuming that the carrier dynamics is quantum-well-like.[6,7,9,12] Therefore, a single activation energy for the carrier escape from coupled, not saturated QD ground states to a quenching channel is introduced. Although such a simplified model roughly describes the temperature dependence of the PL integrated intensity, it does not account for the other features mentioned above. In particular, the model predicts a change in slope between the low- and high-temperature ranges much sharper than the round ''knee'' observed and reported in the literature. In order to take into account the enhanced red shift [item (2)] and the ''knee'' feature, several authors introduced an inhomogeneous broadening in their models, thus representing the QD ensemble as a multiple, decoupled system of QWs. The quenching state has been identified[6,9,10] with the wetting layer, through which excited carriers can reach non radiative recombination centers at the heterostructure interface or in the barrier (alternatively, they can be recaptured by QDs). A rate equation model developed for the multiple QW case[20] has been used, then, with the WL acting the role of the QW barrier and QD parameters being used in place of their QW counterparts. On the contrary, the effect of QD ground-state random population and saturation were not taken into account. The emission intensity of each single dot in the ensemble is given by

$$I_i=P\frac{R_i}{(\beta_i+R_i/U_i)\left[R'+\sum_{j=1}^{n_d}R_j/(\beta_j+R_j/U_j)\right]},\quad (1)$$

where the subscripts i and j stand for different QDs, n_d is the total number of QDs, R_i is the radiative rate of each QD, R' the nonradiative recombination rate in the WL, U_i the trapping rate constants, $\beta_i=\exp(-E_i/kT)$—E_i being the depths of the confined QD states below the WL state, and P is the excitation rate into the WL. Finally, the above equation has been fitted to the PL integrated intensity.[11]

IV. THEORETICAL MODEL

Equation (1) is the basis for the development of an extended set of rate equations modeling the excitation and recombination processes in QDs. In these models, where carriers injected in the barrier at a constant rate by an external excitation source fall in the QDs or recombine nonradiatively directly in the barrier, the role of carrier reservoir, played by the barrier in QWs, is taken by the barrier itself and by the wetting layer. This doubles the number of activation energies and gives rise to a carrier redistribution among the QD levels which is observed much before a substantial quenching of PL takes place[6] and is more important at high temperatures. We model the GaAs barrier, wetting layer, and QD system under optical excitation by the rate-equation scheme shown in Fig. 2.

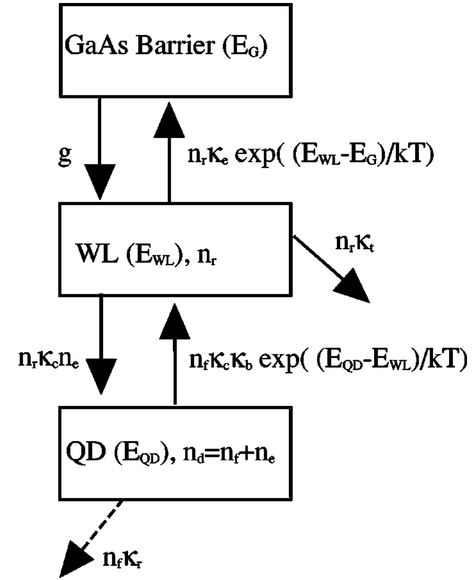

FIG. 2. Schematic representation of the rate equation model described in the text.

The following points determine the set of rate equations.

(1) The external excitation fills a reservoir, the GaAs barrier, from which the excitation is transferred to the WL at rate g.

(2) The direct QD-to-barrier capture/emission channels are not taken into account.

(3) The n_r excitons in the WL are either captured by dots with probability κ_c, or are thermally excited to the barrier at a rate given by $\kappa_e\exp(-\Delta E_{\mathrm{WL\ barrier}}/k_BT)$, or are captured by nonradiative recombination centers with probability κ_t.

(4) Only the ground state of each of the n_d different dots enters the rate equations since only PL from the ground state has been observed in the present experiment, consistently with the low-excitation density used in our experiment. Moreover, QD excited states are usually 50–70 meV higher in energy than the ground state and, therefore, do not contribute to the QD density of occupied states. Their role as an excitation buffer for the QD has been also neglected, mainly because the magnitude of the transition times to the QD ground state is expected to be similar to that of the WL–QD capture process.

(5) The QDs are filled randomly with only one e-h pair and

$$n_d=n_f+n_e,\quad (2)$$

where n_f is the number of filled QDs and n_e that of empty QDs. This assumption is not conflicting with recent reports of biexciton emission from QDs.[21] In fact, the exciton-exciton binding energy is low and the model for the temperature dependence of a doubly degenerate state is almost equivalent to that of two singly degenerate, decoupled states.

(6) Since the process of QD population is intrinsically random,[19] the QD DOS is assumed to be proportional to the low-T PL emission band. This allows us to treat on an equal footing both monomodal and multimodal PL spectra, with no *a priori* assumption on the nature of the QD DOS.

(7) A general consensus has not been reached yet on the correlated or uncorrelated nature of carriers in QDs. In our model carriers are assumed to behave as correlated *e-h* pairs and all dots are neutral, mainly for sake of simplicity. However, in the case of QWs it has been shown that the temperature dependence of the QW photoluminescence is not affected by the band-offset ratio.[20,22] In that case, there is no need of a separate dynamics for electrons and holes for describing thermal quenching and retrapping of carriers. The assumption of a carrier dynamics dominated by coupled *e-h* pairs is quite sound in QDs, where the zero-dimensional confinement gives rise to a strong Coulomb interaction between carriers.[23]

(8) The radiative recombination frequency $\kappa_r \equiv 1/\tau_r$ is the same in all QDs, which are assumed to be defect free, in particular free of nonradiative channels in the bulk and at the interfaces.

(9) The frequency of thermal escape of carriers from the QDs to the WL is given by $\exp(-\Delta E_{\text{QD-WL}}/k_B T)^* \kappa_b \kappa_c$, where κ_b is the effective DOS of the WL. This assumption is consistent with the observation that the density of the WL states is much larger than that of the QD states.

We neglect several expected temperature dependencies of the model parameters. This choice is motivated by our sake of simplicity and by our effort of presenting a model with the lowest number of parameters that still leads to a significant progress in reproducing the experimental data. Therefore, we did not introduce any new parameter, or guessed temperature dependences, unless they sizeably improved our fits.

The rate equations of the QD system are the following:

$$n_d(E) = n_f(E) + n_e(E),$$

$$\dot{n}_f(E) = -n_f(E)\kappa_r - n_f(E)\gamma\kappa_c\kappa_b + n_r n_e(E)\kappa_c = 0, \quad (3)$$

$$\dot{n}_r = g - n_r\kappa_t - n_r\beta\kappa_e + \int n_f(E)\gamma\kappa_c\kappa_b \mathrm{d}E - \int n_r n_e(E)\kappa_c \mathrm{d}E = 0,$$

where $\int n_d(E)\mathrm{d}E = n_d$, $\gamma = \exp(-\Delta E_{\text{QD-WL}}/k_B T)$ and $\beta = \exp(-\Delta E_{WL-barrier}/k_B T)$.

The effect of the introduction of a random population of QDs in the model may be made more clear by considering the case of a δ-like DOS for QDs. In the case of stationary conditions, one ends up with

$$g = (\kappa_t + \kappa_e\beta)n_r + \kappa_r n_f, \quad (4)$$

$$\kappa_c n_d n_r = (\kappa_r + \kappa_c n_r + \gamma\kappa_c\kappa_b)n_f. \quad (5)$$

Equation (4) is the steady-state equation for excitons in the QD+WL system. Equation (5) is similar, but pertains only to the QD system. It contains in the right hand side an additional term ($\kappa_c n_r n_f$) which is induced by the presence in the dot of a single level to accommodate the excitons; see Eq. (2). This last term accounts for an increase of the capture time as the dots are filled and plays a major role in the carrier dynamics only when the number of full dots is a sizeable fraction of the total.

In summary, the present model takes into account three major physical effects neglected by previous models,[8,11] namely, the random nature of the QD population process, the saturation of the QD ground state, and the thermal escape of carriers from QDs into the barrier. The former two processes play an important role in determining the PL spectral dependence on T for different excitation power densities by giving rise to a temperature and size dependent capture probability. This favors the capture of carriers by small, high-energy QDs which, otherwise, should loose their carriers for increasing T before large QDs do. This effect slows down the shift with temperature of the carrier population from small to large QDs. The carrier thermal escape into the barrier gives rise, instead, to an increase in the PL thermal quenching and to a second activation energy, observed at high temperature.

V. EXPERIMENTAL RESULTS

The set of equations (3) has been solved numerically. The QD PL spectrum has been calculated then at different temperatures via the equation $I(E) = A\kappa_r n_f(E)$, where A is a normalization factor.

The model contains eight parameters, namely, $g, n_d, \kappa_r, \kappa_c, \kappa_b, \kappa_t, \kappa_e$, and E_{WL}, some of which fixed to experimentally determined values.

(1) Since the QD density just after the transition is a steeply growing function of the coverage,[4] the QD densities reported in the literature cover a wide range of values, with an upper value of $\approx 10^{11}\text{cm}^{-2}$. In the present work, n_d has been determined for the first set of samples by contact microscopy on uncapped samples grown under the same conditions than those of the capped samples investigated by PL. The n_d value (2×10^{10} cm^{-2}) well agrees with previous findings.[24] Because of the lack of direct measurements, we assumed $n_d = 2\times10^{10}$ cm^{-2} also in the case of the second set of samples. This assumption does not reduce the validity of the model, nevertheless, some care must be paid when comparing the values of the fitting parameters of the two sets of samples. In fact, the dot density enters as a multiplicative factor in various terms of the model rate equations.

(2) It has been shown that, in CW excitation at low temperature, the first excited state can be seen in PL when the excitation $g\tau_r/n_d \gtrsim 0.2$; see Ref. 19. By looking at the onset with excitation power density of the excited state emission and by rescaling this power threshold to the effective power, one gets $g\tau_r/n_d = 0.001$, a value which reproduces well the temperature dependence of the QD PL band. This is not affected by small changes of g, thus confirming that QDs are far from saturation, at least in our experimental conditions. In fact, g determines the relative number of filled dots at $T = 0$ and sizeably affects the QD dynamics only when $n_f \approx n_d$, namely, at excitation much higher than those used here; see Eq. (5).

(3) κ_r and κ_c are related, respectively, to the times for carrier radiative recombination and capture in QDs. Values of 1 ns for κ_r, and of 30 ps for the WL-to-QD capture time κ_c have been used (i.e., the values reported in Refs. 14,16).

In summary, only four parameters, κ_b, κ_t, κ_e, and E_{WL} are let free to vary when fitting the temperature dependence of the PL integrated intensity. In the fitting process, the temperature evolution of the PL spectral line shape provides

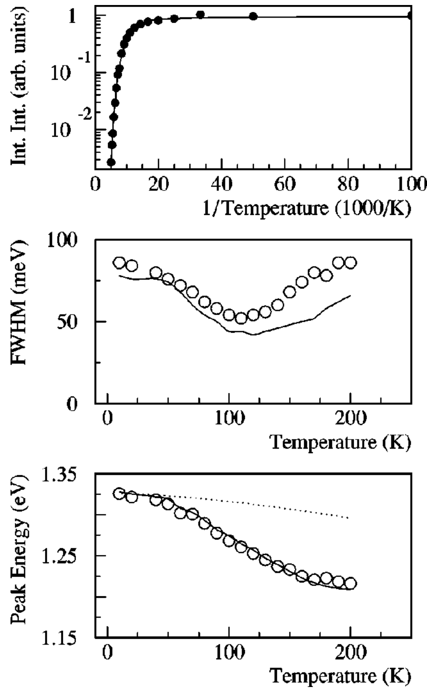

FIG. 3. Integrated PL intensity, FWHM and peak position vs temperature of sample NU1422. The full lines are calculated by solving the set of rate equations 3 with the parameters reported in Table I. The dotted line in the lowest panel shows the InAs gap temperature dependence.

only a criterion for the chi-square minima that prevents the fit from being trapped in an unrealistic local minimum in the parameter space. This criterion is the level of reproduction of the PL spectrum taken at the highest temperature. Model simulations of PL spectra are then calculated by solving Eq. (3) with the parameter values determined by the fit of the integrated intensity.

In Fig. 3, the experimental (symbols) and theoretical simulations (full lines) for the temperature dependence of the integrated intensity, the FWHM, and the peak position are reported for the case of sample NU1422. This sample is characterized by a structured low-T PL band, see Fig. 1, and exhibits, as well as the other two samples in the set, all the anomalous temperature dependencies reported in Sec. III. For increasing temperature, the QD-band shift towards lower energy is faster than that of the InAs band gap, then it slows down thus giving rise to a sigmoidal shape. At the same time, the FWHM of the QD band reduces by $\approx 30-40\,\%$ and reaches a minimum at about 110 K. At higher temperatures the FWHM slowly increases and recovers the low-temperature value at about 200 K. The agreement between experimental data and model simulations goes from good to

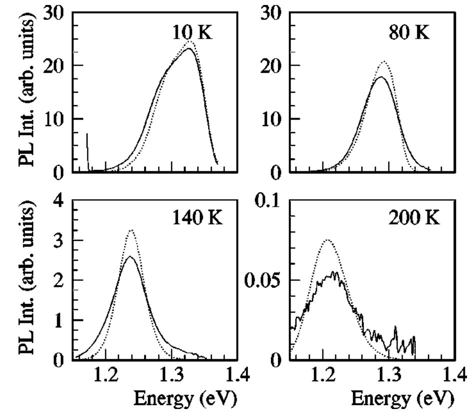

FIG. 4. Experimental (full line) and calculated (dotted line) PL spectra for sample NU1422 at four different temperatures.

excellent, despite the model simplicity. A similar spectral behavior and good degree of data simulation has been achieved also for the other two samples, NU1468 and NU1478, which exhibit a simpler PL-band line shape; see Fig. 1. The values of the parameters entering the PL fits are given in Table I for all samples.

Also the fine-grain characteristics of the PL spectra are accurately reproduced by the present model, as shown in Fig. 4. Therein, the changes of the FWHM and line shape of the PL band produced by the redistribution of carriers among the QD states is quantitatively reproduced. The QD disordered system, not thermalized at low temperature, reaches condition of partial (full) thermalization at intermediate (high) temperatures via the WL. This recovery of thermalization conditions produces the observed shift of weight from the high- to the low-energy side of the PL band.

The present model is validated by a comparison of the WL energy estimated directly, from PL excitation measurements or PL spectra at high power density, with that obtained from the fit of the theoretical model to PL data. In fact, the energy of the WL state critically determines the evolution with temperature of the PL spectra. As a matter of fact, the value of E_{WL} obtained from the fit of sample NU1478 (1.420 ± 0.015 eV, see Table I) perfectly matches the energy of the WL emission (1.420 eV) which appears for exciting power densities on the order of 1 kW cm^{-2}. This supports our assumption of a carrier dynamics dominated by the escape of e-h pairs. In the case of an independent escape of carriers, indeed, the activation energy for carrier escape would be equal to that of the less bound carrier.

In the second set of samples, the WL energy position determined by PLE measurements changes by small amounts (from 1.40 to 1.41 eV, see Table I). Nevertheless, the QD spectrum shows major changes for increasing InAs cover-

TABLE I. Parameters used to fit PL temperature dependencies. Bold numbers indicate fixed parameters. The last column reports the parameter set of sample MA886 when the constraint on κ_e is relaxed.

	NU1468	NU1422	NU1478	MA882	MA884	MA886	MA886 (rel.)
E_{WL} (eV)	1.390 ± 0.015	1.410 ± 0.015	1.420 ± 0.015	**1.410**	**1.406**	**1.400**	**1.400**
κ_t (GHz)	772 ± 230	92 ± 30	138 ± 48	1677 ± 500	3800 ± 1000	3060 ± 750	3300 ± 900
κ_e (10^5 GHz)	5.10 ± 1.60	0.60 ± 0.25	3.80 ± 1.15	130 ± 30	**130**	**130**	450 ± 200
κ_b (10^{17} cm^{-2})	2.7 ± 0.8	4.7 ± 1.4	8.7 ± 2.6	3.8 ± 1.2	10 ± 3	600 ± 180	350 ± 100

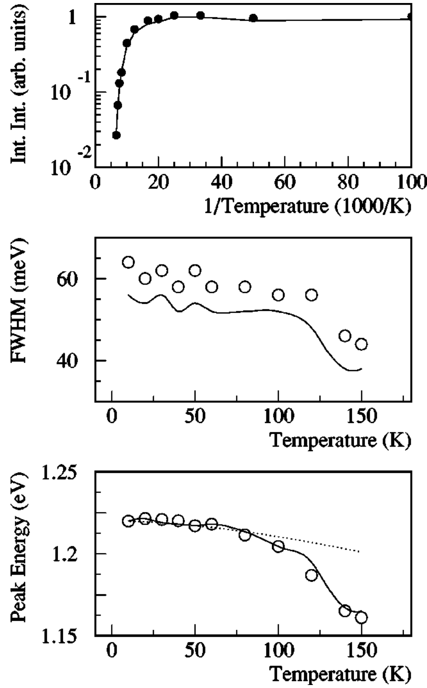

FIG. 5. Integrated PL intensity, FWHM and peak position vs temperature of sample MA886. The full lines are calculated by solving the set of rate equations (3) with the parameters reported in Table I. The dotted line in the lowest panel shows the InAs gap temperature dependence.

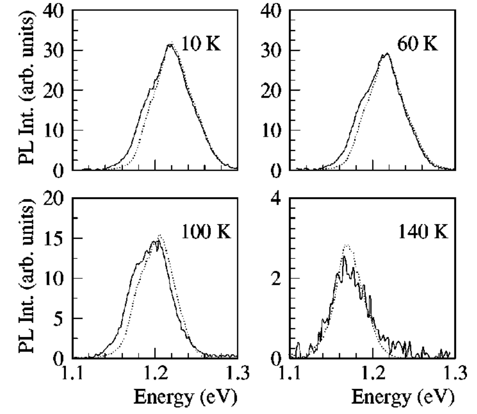

FIG. 6. Experimental (full line) and calculated (dotted line) PL spectra for sample MA886 at four different temperatures.

ages L. Samples MA882 and MA884 ($L=1.6$ and 2.0 ML) show a PL spectrum characterized by a single, Gaussian QD emission band; see Fig. 1. In sample MA886, with a higher In coverage ($L=3.0$ ML), the PL spectrum shows a main peak and a low-energy shoulder whose relative strength increases for increasing temperature. We have fitted the integrated intensity of sample MA882 in terms of three parameters κ_b, κ_t, and κ_e, the WL energy having been fixed to the experimentally determined value. Then, the integrated intensity of the other two samples has been reproduced by using κ_t and κ_b as free parameters, the other two parameters being either given by the PLE results (E_{WL}), or being taken equal to the value derived from the fit of the sample MA882 (κ_e). κ_t and κ_b were let free to vary, instead, in order to take into account the changes from sample to sample of the radiative efficiency and WL DOS. The values of the fitting parameters for this second set of samples are reported in Table I. The fits (full lines) of the PL integrated intensity, FWHM, and peak position for sample MA886 are reported in Fig. 5, together with the experimental data (symbols). The reproduction of the spectral features is fully satisfactory, as found also in the case of sample MA882 (the case of sample MA884 is slightly different, as will be discussed in the following Sec. VI). The rapid temperature shift of the QD-band peak position is followed accurately by the model simulations, as well as that of FWHM (which varies with T less than it was found in the first set of samples). Moreover, the PL spectra as a function of temperature are well reproduced by the model, as shown in Fig. 6 in the case of sample MA886.

VI. DISCUSSION

Despite its simplicity, the model introduced in the previous Sec. V has demonstrated a high degree of prediction and transferability. Besides the six samples reported in this paper, the model has been verified on a wide set of samples (about fifteen) coming from three different sources and grown on substrates with various orientations. In almost all those samples, the agreement between the model simulations and the experimental data is as good as for the samples reported here. The model fails only for some samples ($\approx 10\%$ of the total) which show temperature characteristics different from the general behavior presented in Sec. III. A typical example of such subset is sample MA884. It belongs to the same series of samples MA882 and MA886, but with an InAs coverage of 2.0 ML. The low-T PL of this sample is characterized by a monomodal broad band, see Fig. 1, whose dependence on temperature is that typical of the other samples for what concerns the integrated intensity and peak position, but not for the FWHM. The PL band width does not have a minimum at intermediate temperatures: it remains roughly constant up to 90 K and broadens at higher temperatures, reaching values 30% higher than the low-temperature ones. For what concerns the theoretical model, it accurately fits the dependence of the integrated intensity on temperature and reproduces well the redshift of the peak position. It completely fails, instead, to describe the FWHM temperature dependence. Moreover, the simulated PL spectra only roughly follow the experimental ones. Finally, while the experimental spectrum becomes bimodal at high temperature, the simulated one remains monomodal.

These shortcomings point out a delicate point in the model assumptions, i.e., the determination of the QD DOS on the grounds of low-temperature PL measurements. In fact, the disagreement between the simulated and experimental data might be due to a determinination of the low-energy tail of the QD DOS which is not accurate enough. Indeed, states which are hardly measurable in a PL spectrum at 10 K may become important at higher temperature because of an increased carrier thermalization. As a matter of fact, the agreement between experimental data and model simulations in most (90%) of the samples suggests a description of the carrier quenching process in QDs which is consistent with carrier thermal escape from the ground states of an ensemble

of QDs with different sizes and shapes whose population is not in thermal equilibrium with the lattice. The FWHM reduction and the peak energy rapid redshift with temperature occurring at low-T result from an increase of the carrier thermal emission from small QDs which is not fully compensated by an enhancement of the capture probability induced by random population and ground state saturation effects. The increase in the QD band linewidth observed at higher T's (and the concomitant reduction in the rate of decrease of the QD peak energy vs temperature) is, instead, a consequence of the broadening of the carrier distribution function with increasing temperature. This is confirmed by the observation that the high-T limit of the FWHM is approximately equal to the low-T value. In this context, the temperature dependence of carrier capture and relaxation processes seems to play, instead, a minor role. If one assumes $\kappa_c = \kappa_c^0/T$, namely, a multiphonon transition capture of carriers in QD,[25] no major improvement in the overall quality of the model simulations is obtained.

It is worth to discuss here the values of the four parameters entering the model E_{WL}, κ_t, κ_e, and κ_b, which allowed us to reproduce the PL temperature behavior in a large number of samples, since this may provide a further insight into the photoexcited carrier relaxation and PL quenching processes. In order to compare the numerical values of the whole set of samples on an equal footing, we relaxed the constraint on κ_e while fitting sample MA886. The new parameter values are reported in Table I.

The changes in shape and FWHM of the QD PL band are related to transfer of carriers via the WL. In particular, the value of the energy difference E_{WL} between the WL and the QD ground state is crucial for obtaining the temperature dependence of the PL spectral shape. A change of a few tens of meV in E_{WL} much worsen the agreement between simulated and experimental spectra, thus giving an indirect support to the assumption of a carrier dynamics dominated by correlated *e-h* pairs.

For what concerns κ_t, this parameter widely varies from sample to sample and tends to be lower for samples which exhibit PL emission at higher temperature, since a low quenching probability through the WL increases the high-temperature efficiency. The presence of a superlattice between the substrate and the QD layer helps to prevent the diffusion of dislocations from the substrate and may account for the lower quenching probability through the WL found in the first set of samples with respect to the second set; see Table I.

Another parameter affected by the sample source is the WL to barrier coupling, κ_e, whose value changes by roughly two orders of magnitude on going from the first to the second set of samples. Such differences may be related to the density of defect states accessible from the GaAs barrier.

In the second set of samples, the effective DOS of the WL, κ_b, exhibits a coverage dependence and drops by two orders of magnitude on going from the 3.0 to the 1.6 ML sample. At least part of this drop is due to changes in QD density, whose dependence on InAs coverage[4] is not included in the model.

Finally, it's worth noticing that the the WL-to-QD capture time and the radiative QD recombination lifetime were fixed to the experimental values and that slower decay rates did not give good results. This indirectly supports the observation of a suppression of the theoretically predicted phonon bottleneck reported in time resolved PL experiment.

VII. CONCLUSION

We have presented a system of rate equations for the temperature dependence of the PL in InAs/GaAs QDs which requires a maximum of four free parameters. An excellent agreement between the model simulations of the PL spectra and the experimental results has been obtained for temperatures ranging from 10 to ≈ 150 K in a large number of samples coming from different sources. The theoretical model underlying the rate equations takes into account all the most important mechanisms invoked for explaining the peculiar evolution of the InAs QD-PL band with temperature, namely, carrier thermal escape and retrapping, QD inhomogeneous broadening, random population of the QD ground states, saturation effects, and increasing carrier thermalization for increasing temperature. The mechanism governing the carrier emission is the thermal excitation of correlated *e-h* pairs to the WL state, which acts as transit channel to other QDs or to quenching states inside and/or outside the GaAs barrier. The non monothonic dependence on T of the linewidth and peak energy is accounted for in terms of an increasing carrier thermalization within the QD disordered system and in the WL. Finally, although the microscopic carrier relaxation mechanism cannot be established via the present model, a fast relaxation channel seems to be active in the system.

ACKNOWLEDGMENTS

We acknowledge helpful discussions with M. Colocci, A. Polimeni, and A. Patané. This work has been supported by the Engineering and Physical Sciences Research Council (EPSRC) in the U.K. and partially by the Consiglio Nazionale delle Ricerche (CNR), MADESS project, in Italy. We acknowledge NATO for funds enabling the Milano-Nottingham Collaboration.

[1] G. Bryant, Phys. Rev. B **37**, 8763 (1988).
[2] S. Schmitt-Rink, D. Miller, and D. Chemla, Phys. Rev. B **35**, 8113 (1987).
[3] T. Takagahara, Phys. Rev. B **36**, 9293 (1987).
[4] D. Leonard, K. Pond, and P. M. Petroff, Phys. Rev. B **50**, 11 687 (1994).
[5] D. Bimberg, M. Grundmann, and N. Ledentsov, MRS Bull. **23**, 31 (1998).
[6] L. Brusaferri, S. Sanguinetti, E. Grilli, M. Guzzi, A. Bignazzi, F. Bogani, L. Carraresi, M. Colocci, A. Bosacchi, P. Frigeri, and S. Franchi, Appl. Phys. Lett. **69**, 3354 (1996).
[7] D. I. Lubyshev, P. González-Borrero, J. E. Marega, E. Petitprez, J. N. La Scala, and P. Basmaji, Appl. Phys. Lett. **68**, 205 (1996).
[8] H. Lee, W. Yang, and P. Sercel, Phys. Rev. B **55**, 9757 (1997).
[9] Z. Xu, Z. Lu, X. Yang, Z. Yuan, B. Zheng, J. Xu, W. Ge, Y. Wang, J. Wang, and L. Chang, Phys. Rev. B **54**, 11 528 (1996).

[10] S. Fafard, S. Raymond, G. Wand, R. Leon, D. Leonard, S. Charbonneau, J. Merz, P. Petroff, and J. Bowers, Surf. Sci. **361/362**, 778 (1996).

[11] W. Yang, R. Lowe-Webb, H. Lee, and P. Sercel, Phys. Rev. B **56**, 13 314 (1997).

[12] Y. Wu, K. Arai, and T. Yao, Phys. Rev. B **53**, R10 485 (1996).

[13] R. Heitz, A. Kalburge, Q. Xie, M. Grundmann, P. Chen, A. Hoffmann, A. Madhukar, and D. Bimberg, Phys. Rev. B **57**, 9050 (1998).

[14] B. Ohnesorge, M. Albrecht, J. Oshinowo, A. Forchel, and Y. Arakawa, Phys. Rev. B **54**, 11 532 (1996).

[15] M. Vollmer, E. Mayer, W. Rühle, A. Kurtenbach, and K. Eberl, Phys. Rev. B **54**, R17 292 (1996).

[16] R. Heitz, M. Veit, N. Ledentsov, A. Hoffmann, D. Bimberg, V. Ustinov, P. Kop'ev, and Z. Alferov, Phys. Rev. B **56**, 10 435 (1997).

[17] X. Li and Y. Arakawa, Phys. Rev. B **56**, 10 423 (1997).

[18] A. L. Efros, V. A. Kharchenko, and M. Rosen, Solid State Commun. **93**, 281 (1995).

[19] M. Grundmann and D. Bimberg, Phys. Rev. B **55**, 9740 (1997).

[20] M. Vening, D. Dunstan, and K. Homewood, Phys. Rev. B **48**, 2412 (1993).

[21] A. Kuther, M. Bayer, A. Forchel, A. Gorbunov, V. Timofeev, F. Schäfer, and J. Reithmaier, Phys. Rev. B **58**, 7508 (1998).

[22] J. Lambkin, D. Dunstan, K. Homewood, L. Howard, and M. Emeny, Appl. Phys. Lett. **57**, 1986 (1990).

[23] A. L. Efros, V. Karchenko, and M. Rosen, Solid State Commun. **93**, 281 (1997).

[24] T. R. Ramachandran, R. Heitz, P. Chen, and A. Madhukar, Appl. Phys. Lett. **70**, 640 (1997); **70**, 3169 (1997).

[25] M. Lax, Phys. Rev. **119**, 1502 (1960).